

Ab-initio investigations of novel potential all-d metal Heusler alloys Co₂MnNb

Sumit Kumar^{1,2}[0000-0001-7276-8287], Diwaker³[0000-0002-4155-7417], Vivek Kumar²[0000-0001-7971-0897],
Karan S. Vinayak¹[0000-0002-1380-8370] and Shyam Lal Gupta⁴[0000-0003-0472-3436]

¹ Department of Physics, DAV College Sec-10, Chandigarh – 160010, India

² Department of Physics, Government College Una, H.P. – 174303, India

³ Department of Physics, SCVB Govt. College, Palampur, Kangra, H. P. – 176061, India

⁴ HarishChandra Research Institute (HRI), Prayagraj, U. P. – 211019, India

shyam.lal.gupta@hri.res.in

Abstract. In this study, we employ the Wien2k code to conduct ab-initio study of a novel potential all-d-metal Heusler alloy Co₂MnNb. The analysis utilizes the comparison of local spin density approximations (LDA) with Perdew-Burke-Ernzerh parameterized Generalized Gradient Approximation (PBE-GGA) for structural optimization while modified Becke-Jones potential (mBJ) exchange-correlation potentials to examine various characteristic properties of the alloy under study. Employing Birch-Murnaghan equation of state, we construct the energy-versus-volume curve, facilitating the determination of stable phases and structural parameters of the investigated alloys. Structural optimization in both non-magnetic (NM) and spin-polarized (FM) states reveals the stability of the alloy in the FM state. The compound exhibits metallic behavior in bulk, with notable anisotropic semiconducting behavior for down spin while pure metallic behavior for up spin electrons. Partial density of states of each element of the composition is also analysed to compare their respective contribution towards the observed band structure. The anisotropic behavior of Co₂MnNb for a specific spin state could be of importance in future spintronic and other thin films device applications.

Keywords: Heusler alloy, Density Functional theory (DFT), Crystal and Magnetic Structure, Density of States (DOS)

1 Introduction

Ever-since the inception in 1903 Heusler alloys [1] constitute a remarkable materials class encompassing over > 1000 distinct members, each exhibiting a diverse array of extraordinary properties. Their versatility renders them invaluable across various applications, including spintronics [2, 3, 4, 5], shape memory [6, 7], giant magnetoresistance (GMR) [8, 9], and thermo-electric applications [10, 11, 12, 13]. Despite nearly a century of intensive study, Heusler alloys remain a subject of enduring fascination among scholars, owing to their immense combinatorial potential and wide range of extraordinary properties including half metallicity; ferro and ferri magnets at room temperature and at high temperature. Half metals act as metals for one(up/down) spin type while as insulators or semiconductors for opposite(down/up) spin orientation.

Some materials in half metals exhibit anisotropic behavior for a specific spin. In different directions, they behave as a metal, an insulator, or a semiconductor. The search for Heusler alloys and ferromagnetic semiconductors with stable half-metallicity and high curie temperature is still a daunting task for material science researchers. Since half metallic compounds has special properties based upon direction of spin, so it becomes important to understand the relation between structure and properties to design new materials for the desired functionality. To fulfill this need, computational simulations plays a pivotal role to explore the new compounds and their properties. This will make it easy for experimentalists to narrow down their choices among the wide range of possible materials. The studies of magnetic Heusler compounds designed specifically for spintronic applications paved the way for new possibilities for future. In recent 7-8 years, more than 750 papers are published on full Heusler alloys. Recently, many novel compositions for potential Heusler alloys, Co_2CuAl [14], Co_2NbGe [15], Ir_2VZ ($Z=\text{Sn,In}$)[16], Ir_2CrZ ($Z=\text{Sn,In}$)[17] were investigated via first principle calculations. Junaid Jami et.al.[18] investigated iron based full heusler alloy Fe_2MnSn in all possible phases. Ambrose et.al.[19] made a groundbreaking investigation on Heusler alloy film growth a few years ago by growing a film of Co_2MnGe on the $\text{GaAs}(001)$ substrate. They observed lattice constant enhancement for thin film samples compared to its bulk form. As a result researchers explored Co_2Mn based Heusler alloys for half-metallicity at room temperature. Consequently, Cobalt and Manganese based Heusler alloys becomes center of attraction for researchers to realize room and high temperature half-metallicity. Paula and Reis [20, 21] explained in detail that replacing the p-block element (Z in X_2YZ Heusler alloy) with a transition element increases mechanical ductility and induces large reversible mechano-caloric effects. They highlighted that replacing p-d hybridization with d-d hybridization improves the alloy's mechanical characteristics. Some compositions shows magnetism with high T_c values and following the Slater-Pauling rule. As a result, this effect may broaden the range of spintronic applications. They are commonly known as all-d-metal [21] Heusler alloys. The improved functional behavior reveals them constituting new class of materials for promising state-of-the-art technological applications. In this study, the properties of an all-d-metal novel Heusler alloy Co_2MnNb by first principles using WIEN2K[22] DFT code in fully ordered L2_1 structure in possible antiferromagnetic (AFM) and ferromagnetic configuration(FM).

2 Computational Details

The electronic and magnetic behavior along with the structural properties of Co_2MnNb are reported in this work. The method of full-potential linearized augmented plane-wave (FP-LAPW)[23, 24, 25] implemented within a commercially available DFT [26, 27] based software package named as WIEN2k is used in the present study. We have employed the PBE-GGA and LDA to model and thence to compare these electronic exchange–correlations [28, 29] on structural properties. Fur-

ther to analyze the the band structures(electronic) and electronic DOS more accurately, we have utilized the modified Becke Jones (mBJ) exchange and correlation potential[30]. A k-point grid of 10x10x10 k-mesh distributed over the Brillouin zone (BZ), value of 9.0 for product $RMT \times K_{max}$, and that of 2.18, 2.18, and 2.13 (a.u) are used as non-overlapping muffin-tin radii for Co, Mn, and Nb, respectively. While G_{max} is set as 12, the energy cutoff (core) of -8.0 Ryd was chosen to define the separation of valence and core states. The convergence limit of 10-4 Ry is used for performing these self consistent calculations. The ground state energy for the ferromagnetic (FM) phase and all possible antiferromagnetic structures are investigated in $L2_1$ structure. Furthermore, we also report the fraction of spin polarization (SP) in percentage as given by[31, 32]

$$SP = \frac{\eta \uparrow - \eta \downarrow}{\eta \uparrow + \eta \downarrow} \times 100 \quad (1)$$

where $\eta \uparrow$ and $\eta \downarrow$ represent the majority and minority spin states.

3 Results and Discussion

3.1 Structural Properties

To determine the ground state energy of Co_2MnNb , we have evaluated non-magnetic (NM), antiferro-magnetic (AFM) alongwith ferro-magnetic (FM) phases in cubic $L2_1$ structure. For the AFM phase, we investigated all six possible spin configurations for ground state energy: udu (Co-up, Mn-down, and Nb-up), dud, uud, ddu, udd, and duu. The conventional unit cells of the above phases employed to carry out the computations is depicted in Fig. 1. X-crysden package [33] is used to visualize the crystal structure.

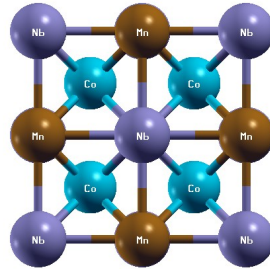


Fig. 1. Co_2MnNb in $L2_1$ structure (Fm-3m space group)

PBE-GGA and LDA exchange-correlation potentials are used to investigate the ground state energy and volume optimization in NM, AFM and FM phases. Birch Murunaghan equation of state is then used to fitting the variations of obtained total energy of the system with its volume and thence to get the optimized values of vari-

ous parameters including the lattice constant as given in Table – 1. Total Energy vs Volume curve of Co_2MnNb alloy in PBE-GGA and LDA for NM and FM phases are shown in Fig. 2 and Fig. 3 respectively. Among all the investigated phases, FM phase in L_2 structure is the energetically most favorable with lattice constant of 5.9723\AA with -15532.2116 Ryd. This structure with the lowest energy spin configuration is then further investigated for other properties.

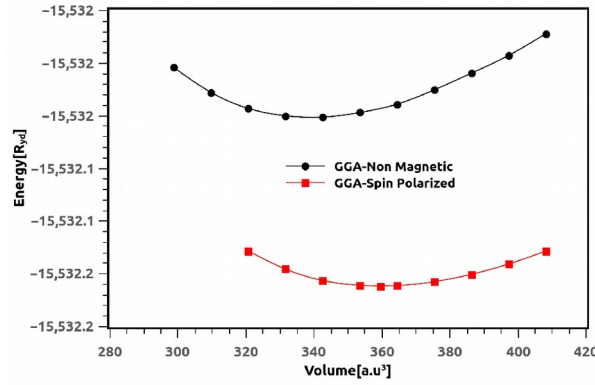


Fig. 2. Volume optimization in GGA

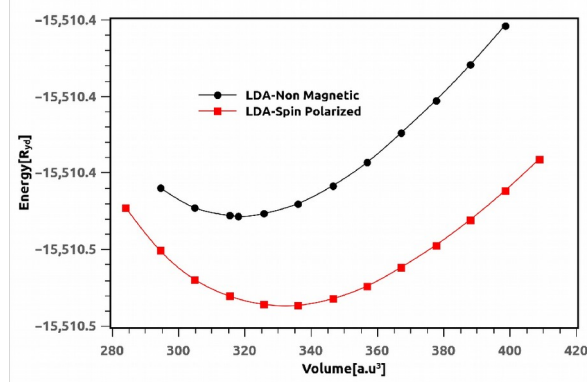


Fig. 3. Volume optimization in LDA

The formation energy of Co_2MnNb alloy is further predicted as following for analyzing its thermodynamic stability,

$$\Delta H_f = E_{\text{tot}} - (2x E_{\text{Co}} + E_{\text{Mn}} + E_{\text{Nb}}) \quad (2)$$

where the term E_{tot} represents the total energy of ground state of the compound Co_2MnNb per formula unit and the terms E_{Co} , E_{Mn} and E_{Nb} represent the total ground state energies for the bulk Co, Mn and Nb respectively. Using the calculated values of respected energies in equation-2, we found ΔH as -1.51ev/f.u. which indicates its phase stability.

Table 1. Calculated parameters for Co₂MnNb in different phases

Phase (XC Potential)	Structure	Bulk modulus (GPa)	Latt. Constant (Å°)	Tot. Energy (Ry)	Volume (a.u. ³)
FM (GGA)	L2 ₁	188.4249	5.9723	-15532.2116	359.3856
NM (GGA)	L2 ₁	232.7926	5.8547	-15532.0474	338.5679
FM (LDA)	L2 ₁	220.1766	5.8105	-15510.5369	330.9571
NM (LDA)	L2 ₁	272.7349	5.7344	-15510.4782	318.1289
AFM-udu (GGA)	L2 ₁	185.3116	5.9754	-15532.2114	359.9545
AFM-dud (GGA)	L2 ₁	183.3883	5.9727	-15532.2111	359.4508
AFM-uud (GGA)	L2 ₁	185.9791	5.9745	-15532.2115	359.7883
AFM-ddu (GGA)	L2 ₁	186.3019	5.9734	-15532.2115	359.5896
AFM-udd (GGA)	L2 ₁	186.0180	5.9737	-15532.2115	359.6339
AFM-duu (GGA)	L2 ₁	187.8176	5.9730	-15532.2115	359.5162

3.2 Electronic and Magnetic Properties

Fig. 4 and Fig. 5 depict the calculated total and projected DOS for the FM phase within the L2₁ structure while Fig. 6 and Fig. 7 show the respective band structures (electronic) for majority as well as minority spins. The asymmetric distribution among those spins depicts the magnetic nature and exhibit lack of complete spin polarization at the Fermi energy E_F . The projected DOS (pDOS) plots (see Fig. 4 and Fig. 5) establish Co and Mn as primary contributors compare to Nb having negligible contribution towards total DOS. The broad spectrum of d states of majority spins is attributed to hybridization of d-states among Co, Mn and Nb atoms. An analysis of the band structure for the majority spin channel (see Fig. 6) echoes the metallic behavior generated by the fusion of conduction and valence bands. The analysis of minority spins (see Fig. 7) indicates a semiconducting gap at zone center Γ and along symmetry direction L, while a slight merger of valence and conduction bands around the rest of the symmetry directions, leading to a bulk metallic behavior.

As anticipated, the total magnetic moment (see Table-2) in the FM L2₁ structure ($6.0656\mu_B$) predominantly originates from the two symmetrically equivalent Co atoms (each Co atom contributing $1.5391\mu_B$) and the Mn atom (contributing $3.4946\mu_B$), with the Nb atom exhibiting a negligible induced negative magnetic moment. Closer look into Table - 2 indicates that Slater Pauling rule is not being followed in Co₂MnNb. The Slater Pauling rule demands $M = (N_V - 24) \mu_B$, where M represents the net magnetic moment while N_V is the total number of valence electrons in a unit cell. Each unit cell in Co₂MnNb has 28 valence electrons.

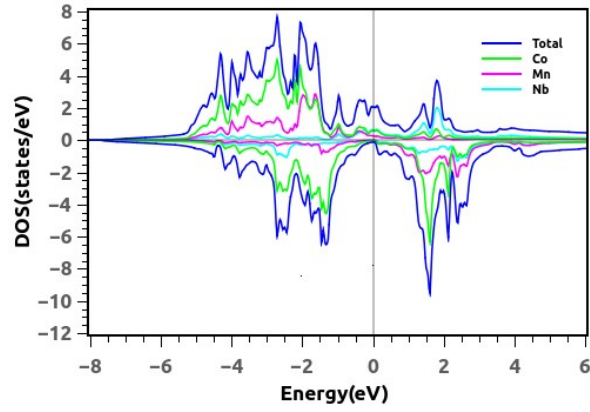


Fig. 4. Spin polarized total and projected DOS

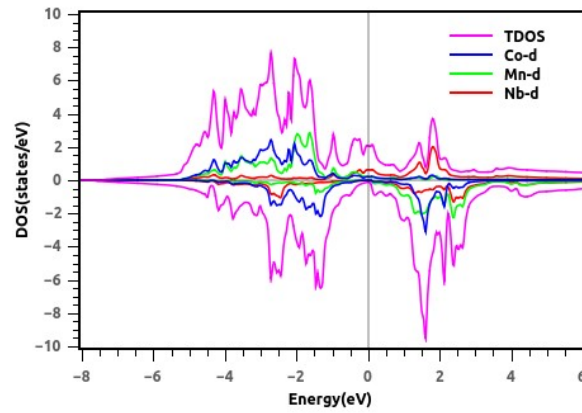


Fig. 5. Spin polarized total and d-orbital DOS

The magnetic moment should be 4 (Slater-Pauling rule); however the obtained larger magnetic moment indicates the presence of other interactions namely spin-orbit interactions controlling the magnetic behavior.

4 Conclusion

Within the sprawling compositional spectrum of full Heusler alloys, first-principles computations are the most feasible method to predict experimentally realizing specific composition with desired properties. The adopted pathway via DFT based WIEN2K

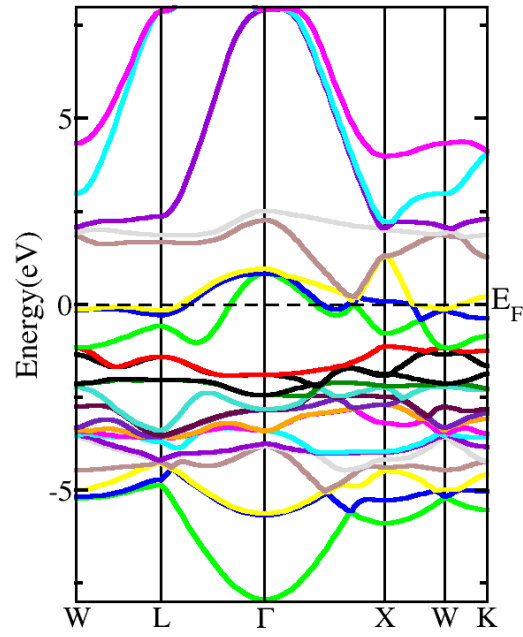


Fig. 6. Band structure of Co₂MnNb (Spin-Up)

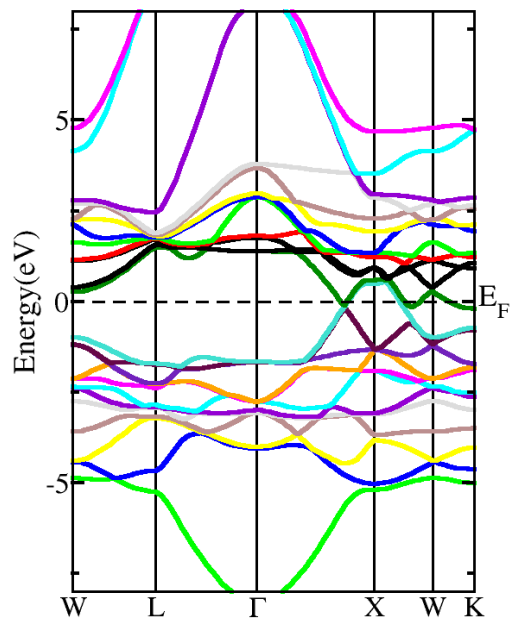


Fig. 7. Band structure of Co₂MnNb (Spin-Down)

Table 2. Total and partial magnetic moments of Co₂MnNb

Quantity per unit cell	Value in μ_B
μ_{tot}	6.0656 (mBJ)
	5.9503 (GGA)
	5.7358 (LDA)
μ_{Co}	1.5391 (mBJ)
	1.3245 (GGA)
	1.2472 (LDA)
μ_{Mn}	3.4946 (mBJ)
	3.3365 (GGA)
	3.0983 (LDA)
μ_{Nb}	-0.1697 (mBJ)
	-0.0558 (GGA)
	-0.0048 (LDA)

software package in this study entails a step wise identification of the theoretically most stable crystal and magnetic structure. The FM state of the cubic L2₁ structure is found to be the energetically most stable with net magnetic moment of $6.056\mu_B$ per formula unit, primarily originating from Co and Mn constituent atoms. The detailed DOS analysis indicate role of the hybridization of d-orbitals towards the magnetic behavior. The TDOS confirmed the metallic behavior of the compound with spin polarization of 85.67 percent at E_F . The DOSs and band structures show that the bulk behaviour of the novel potential Heusler alloy under investigation is metallic for the majority spins and anisotropic behaviour (semiconducting gap at Γ center and L direction whereas metallic in other high symmetry directions) for the minority spin channel. This anisotropic Co₂MnNb behavior for a specific spin may be crucial in spintronic devices. Additional investigations into phonon behavior, magnetic anisotropy and exchange interactions along with thermodynamic properties will be required in order to explore and establish the studied composition as technologically important and viable Heusler alloy.

References

1. Heusler, F; Ueber magnetische Manganlegierungen. Verhandlungen Dtsch. Phys. Ges. 5, 219 (1903).

2. Casper F., Graf T., Chadov S., Balke B., Felser C.; Half-Heusler compounds: novel materials for energy and spintronic applications. *Semiconductor Science and Technology* 27, 063001 (2012).
3. Lashkerav G. V., Radchenko M. V., Karpina V. A., Sichkovsky V. I.; Diluted ferromagnetic semiconductors as spintronic materials. *Low Temp. Phys.* 33, 165 (2007).
4. Xu J.; First principles study of III-V diluted magnetic semiconductors. *Dissertations Abstracts International* 68, 7610 (2007).
5. Dietl T.; Origin of ferromagnetic response in diluted magnetic semiconductors and oxides. *J Phys. Cond. Matter.* 19,165204 (2007).
6. Ma Y.Q., Jiang C.B., Li Y., Wang C.P., Liu X.J.; Heusler Type CoNiGa Alloys with High Martensitic Transformation Temperature. *Mater. Sci. Forum* 546, 2241 (2007).
7. Pons J., Cesari E., Segui C., Mssdue F., Santamarta R.; Ferromagnetic shape memory alloys: Alternatives to Ni-Mn-Ga. *Mater. Sci. Eng. A* 481, 65 (2008).
8. Baibich M.N., Broto J.M., Fert A., Nguyen Van Dau F., Petroff F., Etienne P., Creuzet G., Friederich A., Chazelas J.; Giant Magnetoresistance of (001)Fe/(001)Cr Magnetic Superlattices. *Phys Rev Lett.* 61, 2472 (1988).
9. Binash G., Grunberg P., Saurenbach F., Zinn W.; Enhanced magnetoresistance in layered magnetic structures with antiferromagnetic interlayer exchange. *Phys. Rev. B* 39, 4828 (R) (1989).
10. Graf T., Felser C., Parkin S.S.P.; Simple rules for the understanding of Heusler compounds. *Prog. Solid State Chem.* 39, 1 (2011).
11. Krishnaveni S., Sundareswari M.; Band gap engineering in ruthenium-based Heusler alloys for thermoelectric applications. *Int. J. Energy Res Mater. Trans.* 55, 1209 (2014).
12. Krishnaveni S., Sundareswari M., Deshmukh P.C., Velluri S.R., Roberts K.; Band structure and transport studies of half Heusler compound DyPdBi: An efficient thermoelectric material. *J. Mater. Res.* 31, 15 (2016).
13. Balke B., Fecher G.H., Felser C.; New heusler compounds and their properties Spintronics: From Materials to Devices. *Springer Science Business Media Dordrecht* 15, 43 (2013).
14. Kumar S., Diwaker, Gupta S.L., Kumar D., Vinayak K.S.; Ab initio study of the newly proposed full Heusler alloy Co₂CuAl : Insights from DFT. *Materials Today:Proceedings*, (2023) <https://doi.org/10.1016/j.matpr.2023.03.105>.
15. Kumar S., Diwaker, Gupta S. L., Kumar D., Vinayak K. S.; Structural properties of novel potential spintronic material and Full-Heusler alloy Co₂NbGe: First Principles investigation. *Materials Today:Proceedings*, (2022), <https://doi.org/10.1016/j.matpr.2022.11.122>.
16. Gupta S. L., Kumar S., Anupam, Thakur S. S., Panwar S., Diwaker; A newly proposed full Heusler alloy Ir₂VZ(Z = Sn, In) suitable for high-temperature thermoelectric applications: A DFT approach. *Mod. Phys. Lett. B* 38(09), 2450030 (2024).
17. Gupta S. L., Singh S., Kumar S., Anupam, Thakur S. S., Kumar A., Panwar S., Diwaker; Ab-Initio stability of Iridium based newly proposed full and quaternary heusler alloys. *Physica B: Condensed Matter* 674, 415539, (2024).
18. Jami J., Pathak R., Venkataramani N., Suresh K. G., Bhattacharya A.; First-principles investigation of the structure, stability, and magnetic properties of the Heusler alloy. *Phys. Rev. B* 108, 054431 (2023).

19. Ambrose T., Krebs J. J., Prinz G.A.; Epitaxial growth and magnetic properties of single-crystal Co₂MnGe Heusler alloy films on GaAs(001). *Appl Phys Lett.* 76, 3280 (2000).
20. de-Paula V. G., Reis M. S.; All-*d*-Metal *Full* Heusler Alloys: A Novel Class of Functional Materials. *Chem. Mater.* 33(14), 5483, (2021).
21. Wei Z. Y., Liu E. K., Chen J. H., Li Y. Liu G. D., Luo H. Z., Xi X. K., Zhang H. W., Wang W. H., Wu G. H.; Realization of multifunctional shape memory ferromagnets in all-*d*-metal Heusler phases. *Appl. Phys. Lett.* 107(2), 022406 (2015).
22. Blaha P., Schwarz K., Tran F., Laskowski R., Madsen G. K. H., Marks L. D.; WIEN2k: An APW+lo program for calculating the properties of solids. *J. Chem. Phys.* 152, 074101 (2020).
23. Kohn W., Sham L.; Self-Consistent Equations Including Exchange and Correlation Effects. *Phys. Rev.* 140, A1133 (1965).
24. Slater J. C.; Wave Functions in a Periodic Potential. *Phys. Rev.* 51, 846 (1937).
25. Singh D.; Ground-state properties of lanthanum: Treatment of extended-core states. *Phys. Rev. B* 43, 6388 (1991).
26. Shen Q., Chen L., Goto T., Hirai T., Yang J., Meisner G., Uher C.; Effects of partial substitution of Ni by Pd on the thermoelectric properties of ZrNiSn-based half-Heusler compounds. *Appl. Phys. Lett.* 79, 4165 (2001).
27. Hohenberg P., Kohn W.; Inhomogeneous Electron Gas. *Phys. Rev.* 136, B864 (1964).
28. Blaha P., Schwarz K., Madsen G. K., Kvasnicka D., Luitz J.; Wien2K: An Augmented Plane Wave Local Orbitals Program for Calculating Crystal Properties. (2001).
29. Shorikov A. O., Gapontsev V. V., Streltsov S. V., Anisimov V. I.; Doping induced spin state transition in Li_xCoO₂ as studied by the GGA+DMFT calculations. *JETP Lett. (Engl. - Transl.)* 104, 398 (2016).
30. Tran F., Blaha P.; Accurate Band Gaps of Semiconductors and Insulators with a Semilocal Exchange-Correlation Potential. *Phys. Rev. Lett.* 102, 226401 (2012).
31. Soulen Jr. R. J., Byers J., Osofsky M. Nadgorny B., Ambrose T., Cheng S., Broussard P.R., Tanaka C., Nowak J., Moodera J., Barry A., Coey J.; Measuring the Spin Polarization of a Metal with a Superconducting Point Contact. *Science* 282(5386), 85 (1998).
32. I. I. Mazin; How to Define and Calculate the Degree of Spin Polarization in Ferromagnets. *Phys. Rev. Lett.* 83, 1427 (1999).
33. Kokalj A.; XCrySDen—a new program for displaying crystalline structures and electron densities. *J. Mol. Graphics Modelling* 17, 176 (1999).